INTERNATIONAL JOURNAL OF
NUMERICAL ANALYSIS AND MODELING
Volume 3, Number 3, Pages 322–332

SUPERCONVERGENCE STUDIES OF QUADRILATERAL NONCONFORMING ROTATED Q_1 ELEMENTS

PINGBING MING, ZHONG-CI SHI AND YUN XU

(Communicated by Zhimin Zhang)

Abstract. For the nonconforming rotated Q_1 element over a mildly distorted quadrilateral mesh, we propose a superconvergence property at the element center, the vertices and the midpoints of four edges. Numerics are presented to confirm this observation.

Key Words. Superconvergence, Nonconforming rotated Q_1 element, Kershaw mesh.

1. Introduction

Nonconforming rotated Q_1 element [21] (NRQ_1) with mean integral over edges as degrees of freedom (NRQ_1^a) has been widely used in several fields including the computational fluids [21, 25], the crystalline microstructure [11, 13], the Chapman-Ferraro problem [12], the Reissner-Mindlin plate bending problem [16], and the streamline-diffusion problem [22, 24]. Compared with the standard bilinear element, NRQ_1^a exhibits better stability in these problems.

A new NRQ_1 element introduced by Ming and Shi leads to a truly locking-free Reissner-Mindlin plate element over general quadrilateral meshes [19]. Compared to NRQ_1^a, this element has an extra degree of freedom (we call it the five-point NRQ_1, see Definition 2.3). A similar element was presented in [4] to approximate Navier-Stokes equations.

The convergence rate in the energy norm of both NRQ_1 elements is of first order over a rectangular mesh [11, 21]. As to the general quadrilateral mesh, the five-point NRQ_1 retains the first order convergence rate, while NRQ_1^a converges with first order if the mesh is mildly distorted [15, 17]. An example is given to show the first order optimality [15].

Meanwhile, a superconvergence property at element center on the rectangular parallelopiped mesh was obtained for NRQ_1^a [11]. For the mildly distorted quadrilateral mesh, we proved [20] that the supercovergence property is valid not only for the element center, but also for the vertices and midpoints of four edges. Therefore, both elements share the same superconvergence points as the bilinear element [5]. Extensive numerics will be presented in this paper to confirm the theoretic prediction. The same phenomenon was also numerically observed for another NRQ_1 element that employs midpoints value of each edge as degrees of freedom, however,

Received by the editors July 31, 2004 and, in revised form, March 30, 2005.
2000 *Mathematics Subject Classification.* 35R35, 49J40, 60G40.
This research Ming was supported by Research Foundation Of Education Department 6758700 and partly supported by Chinese Natural Science Foundation through 10201033.

there is no theoretic support up to now. Some superclose results for the rectangular NRQ$_1$ element and its variants can be found in [2, 14, 15, 22].

The outline of this paper is as follows. In the next section, we introduce NRQ$_1^a$, NRQ$_1^p$, and the five-point NRQ$_1$ element, the quadrilateral mesh conditions. The main results are stated in § 3. Numerical results and discussion are given in the last section.

2. Nonconforming Rotated $\mathbf{Q}_1$ Element

For any convex polygon Ω, we use the standard Sobolev space $W^{k,p}(\Omega)$ [1]. Denote by $⨍_{\Omega_1} f$ the mean value of a function f over the sub-domain Ω_1 of Ω.

We consider the general second order elliptic boundary value problem

$$\begin{cases} -\partial_x\big(a_{11}\partial_x u\big) - \partial_x\big(a_{12}\partial_y u\big) - \partial_y\big(a_{21}\partial_x u\big) - \partial_y\big(a_{22}\partial_y u\big) = f & \text{in} \quad \Omega, \\ u = 0 & \text{on} \quad \partial\Omega, \end{cases} \tag{2.1}$$

where $\{a_{ij}\}_{i,j=1}^2 \in W^{2,\infty}(\Omega)$, and

$$\lambda |\,\xi\,|^2 \leq \sum_{i,j=1}^{2} a_{ij}\xi_i\xi_j \leq \Lambda |\,\xi\,|^2 \quad \text{for all } \ \xi \in \mathbb{R}^2.$$

Let $\mathcal{T}_h$ be a partition of $\overline{\Omega}$ by convex quadrilaterals K with the mesh size h_K and $h := \max_{K\in\mathcal{T}_h} h_K$. We assume that $\mathcal{T}_h$ is shape regular in the sense of Ciarlet-Raviart [6, p. 247]. Namely, all quadrilaterals are convex and there exist constants $\rho_1 \geq 1$ and $0 < \rho_2 < 1$ such that

$$h_K/\underline{h}_K \leq \rho_1, \qquad |\cos\theta_{i,K}\,| \leq \rho_2, \quad i = 1,2,3,4 \quad \text{for all } \ K \in \mathcal{T}_h.$$

Here h_K, $\underline{h}_K$ and $\theta_{i,K}$ denote the diameter, the shortest length of sides, and the interior angles of K, respectively.

We introduce a mesh condition which quantifies the deviation of a quadrilateral from a parallelogram.

Definition 2.1. $(1+\alpha)$-section condition $(0 \leq \alpha \leq 1)$ [18] *The distance d_K between the midpoints of two diagonals of $K \in \mathcal{T}_h$ is of order $\mathcal{O}(h_K^{1+\alpha})$ uniformly for all elements K as $h \to 0$.*

The extreme case $\alpha = 0$ represents an unstructured quadrilateral mesh subdivision. The mesh partition in Fig. 4 is a particular one, which consists of trapezoids generating from a typical trapezoid with translation and dilation. In case of $\alpha = 1$, the mesh satisfies the *Bi-section condition* [23], which is also the 1-strongly regular mesh [27].

Definition 2.2. *For every element $K \in \mathcal{T}_h$, we call K satisfies the $(1+\beta_K)$-uniform condition if for every elements $K^* \in S(K)$, there exist constants $\beta_1(K^*)$ and $\beta_2(K^*)$ such that*

$$\begin{aligned} |\,\overrightarrow{M_1M_3} - \overrightarrow{M_3M_6}\,| &= \mathcal{O}(h_K^{1+\beta_1(K^*)} + h_{K^*}^{1+\beta_1(K^*)}), \\ |\,\overrightarrow{M_2M_4} - \overrightarrow{M_5M_7}\,| &= \mathcal{O}(h_K^{1+\beta_2(K^*)} + h_{K^*}^{1+\beta_2(K^*)}). \end{aligned} \tag{2.2}$$

We define β_K as

$$\beta_K\!:= \min_{K^*\in S(K)} \min(\beta_1(K^*), \beta_2(K^*)),$$

where $S(K)$ is the subset of $\mathcal{T}_h$ with nonempty intersection with $\overline{K}$, and we refer to Fig. 1 *for M_1M_3, M_3M_6 and M_2M_4, M_5M_7.*

We call $\mathcal{T}_h$ satisfies the $(1+\beta)$-uniform condition if every element $K \in \mathcal{T}_h$ satisfies the $(1+\beta_K)$-uniform condition, where $\beta := \min_{K\in\mathcal{T}_h} \beta_K$.

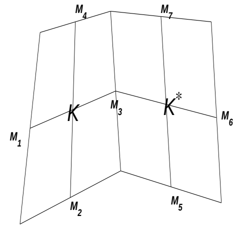

FIGURE 1. $(1+\beta_K)$-uniform mesh

Let $\hat{K}$ be the unit square $(-1,1)^2$ and the bilinear function F_K be an isomorphism from $\hat{K} \to K = F_K(\hat{K})$.

Rannacher and Turek introduced NRQ_1 element [21], which is defined as

$$X_h := \{\, v \in L^2(\Omega) \mid v_{|K} \in \mathcal{Q}_1,\ v \text{ is continuous regarding } Q_e \text{ and } Q_e(v) = 0 \text{ if } e \subset \partial\Omega \,\}, \tag{2.3}$$

where

$$\mathcal{Q}_1 := \{\, q \circ F_K^{-1} \mid q \in \mathrm{Span}\langle 1, \hat{x}, \hat{y}, \hat{x}^2 - \hat{y}^2 \rangle \,\},$$

and $Q_e(v) := ⨍_e v$ for a smooth function $v : K \to \mathbb{R}$ and $e \subset \partial K$.

For any $v \in X_h$, define

$$\|v\|_{l,p,h}^2 = \sum_{K\in\mathcal{T}_h} \|v\|_{l,p,K}^2, \qquad |\, v\,|_{l,h}^2 = \sum_{K\in\mathcal{T}_h} |\, v\,|_{l,p,K}^2, \qquad l = 1,2 \text{ and } 1 \le p \le \infty.$$

It is seen that $|\cdot|_{1,2,h}$ is a norm on X_h.

Denote by Π the standard interpolation operator over X_h. If $\mathcal{T}_h$ satisfies the $(1+\alpha)$-*section condition*, then for each $v \in H_0^1(\Omega) \cap W^{2,\infty}(\Omega)$, using the general theory in [3], we have the interpolation error estimate

$$\|v - \Pi v\|_{L^\infty(\Omega)} + h\|v - \Pi v\|_{1,\infty,h} \le C(h|\, v\,|_{2,\infty} + h^\alpha |\, v\,|_{1,\infty}). \tag{2.4}$$

Observe that the interpolation error degenerates if $\alpha = 0$. To avoid such degradation, similar to [4], we define

Definition 2.3.

$$X_h := \{\, v \in L^2(\Omega) \mid v_{|K} \in \widehat{\mathcal{Q}}_1, v \textit{ is continuous regarding } Q_e \textit{ and } \int_{\hat{K}} (v \circ F_K)\hat{x}\hat{y} = 1 \textit{ and } Q_e(v) = 0 \textit{ if } e \subset \partial\Omega \,\} \tag{2.5}$$

with $\widehat{\mathcal{Q}}_1 := \{\, q \circ F_K^{-1} \mid q \in \mathit{Span}\langle 1, \hat{x}, \hat{y}, \hat{x}\hat{y}, \hat{x}^2 - \hat{y}^2 \rangle \,\}$.

Another version of NRQ_1 is also introduced in [21], which uses midpoints of four edges as degrees of freedoms. We call this element as NRQ_1^p, the one defined in (2.3) as NRQ_1^a and the one defined in (2.5) as the five-point NRQ_1.

The variational problem of (2.1) is to find $u \in H_0^1(\Omega)$ such that

$$a(u,v) = (f,v) \quad \text{for all } v \in H_0^1(\Omega), \tag{2.6}$$

where the bilinear form a is defined for each $v, w \in H_0^1(\Omega)$ as

$$a(v,w) := \int_\Omega (a_{11}\partial_x u \partial_x v + a_{12}\partial_y u \partial_x v + a_{21}\partial_y u \partial_x v + a_{22}\partial_y u \partial_y v)\, dx\, dy.$$

The finite element solution $u_h \in X_h$ satisfies

$$a_h(u_h, v) = (f, v) \quad \text{for all } \ v \in X_h, \tag{2.7}$$

where a_h is defined piecewise for each $v, w \in X_h$ as

$$a_h(v, w) := \sum_{K \in \mathcal{T}_h} \int_K (a_{11}\partial_x u \partial_x v + a_{12}\partial_y u \partial_x v + a_{21}\partial_y u \partial_x v + a_{22}\partial_y u \partial_y v)\, dx\, dy,$$

where X_h is NRQ$_1^a$ or the five-point NRQ$_1$.

3. Main Results

The main results of this paper are

Theorem 3.1. *Let u be the solution of* (2.6)*, and $u_h \in X_h$(NRQ$_1^a$) be the solution of* (2.7)*. We assume that $u \in W^{3,\infty}(\Omega)$ and $\mathcal{T}_h$ satisfies the* $(1+\alpha)$-section condition.

If z is the element center, then

$$|\,\nabla(u - u_h)(z)\,| \le Ch^{2\alpha} |\ln h\,| \, \|u\|_{3,\infty}. \tag{3.1}$$

If z are vertices or midpoints of each edges of the element K, and if K satisfies the $(1+\beta_K)$-uniform condition*, then*

$$|\,\overline{\nabla}(u - u_h)(z)\,| \le C\big(h^{2\alpha} |\ln h\,| + h^{\alpha+\beta_K}\big) \|u\|_{3,\infty}, \tag{3.2}$$

where $\overline{\nabla}$ refers to taking average over all neighboring elements around z.

This theorem is proved in [20, Theorem 2.5], which also holds for many variants of other quadrilateral nonconforming elements, e.g. [7, 9][1]

As to the five-point NRQ$_1$, we have

Theorem 3.2. *Under the same condition of Theorem 3.1 and u_h belongs to the five-point NRQ$_1$, we have*

If z is the element center, then

$$|\,\nabla(u - u_h)(z)\,| \le Ch^{1+\alpha} |\ln h\,| \|u\|_{3,\infty}. \tag{3.3}$$

If z are vertices or midpoints of each edges of the element K, and if K satisfies the $(1+\beta_K)$-uniform condition, then

$$|\,\overline{\nabla}(u - u_h)(z)\,| \le C\big(h^{1+\alpha} |\ln h\,| + h^{1+\beta_K}\big) \|u\|_{3,\infty}. \tag{3.4}$$

This theorem is proved in [20, Theorem 2.6].

Another standard measurement of the error is the discrete ℓ^2 norm $\|\cdot\|_{\ell^2}$, which is defined as

$$\|\overline{\nabla}(u - u_h)(Z)\|_{\ell^2} := (\#Z)^{-1/2} \Big(\sum_{z \in Z} |\,\overline{\nabla}(u - u_h)(z)\,|^2 \Big)^{1/2},$$

where Z may be the element center, the vertices and the midpoints of each edges, and $\#Z$ denotes the number of elements in Z.

Theorem 3.1 and Theorem 3.2 require the $(1+\beta_K)$-uniform condition around the points of interest. For an unstructured mesh, an adaptive mesh refinement will usually bring in such kind of local structure (e.g. diagonal swapping and Lagrange smoothing). However, such local structure usually cannot be retained over the whole triangulation, in particular for elements near the boundary or near the discontinuous line of the coefficients. It is thus reasonable to assume the following condition:

[1] Notice that elements proposed in [7, 9] are rectangular, which can be directly extended to a quadrilateral mesh.

Definition 3.3. *The triangulation $\mathcal{T}_h = \mathcal{T}_{1,h} \cup \mathcal{T}_{2,h}$ is said to satisfy the* Condition (β, σ) *if there exist nonnegative constants β and σ such that every element inside $\mathcal{T}_{1,h}$ satisfies the* $(1+\beta)$-uniform condition *and*

$$\overline{\Omega}_{1,h} \cup \overline{\Omega}_{2,h} = \overline{\Omega}, \quad |\,\Omega_{2,h}\,| = \mathcal{O}(h^\sigma), \quad \overline{\Omega}_{i,h} = \sum_{K \in \mathcal{T}_{i,h}} \overline{K},\ i = 1, 2.$$

Remark 3.4. *A similar condition for a triangular mesh was appeared in* [26].

Corollary 3.5. *If $\mathcal{T}_h$ satisfies the* $(1+\alpha)$-section condition, *then*

$$\|\nabla(u - u_h)(z)\|_{\ell^2} \leq \begin{cases} Ch^{2\alpha}|\ln h\,| & \mathrm{NRQ}_1^a, \\ Ch^{1+\alpha}|\ln h\,| & \text{FIVE-POINT } \mathrm{NRQ}_1 \end{cases}$$

for z being the element center.

If, in addition, $\mathcal{T}_h$ satisfies the Condition (β, σ), *then*

$$\|\overline{\nabla}(u - u_h)(z)\|_{\ell^2} \leq \begin{cases} C(h^{2\alpha}|\ln h\,| + h^{\alpha+\beta} + h^{1+\sigma/2}|\ln h\,|) & \mathrm{NRQ}_1^a, \\ C(h^{1+\alpha}|\ln h\,| + h^{1+\beta} + h^{1+\sigma/2}|\ln h\,|) & \text{FIVE-POINT } \mathrm{NRQ}_1 \end{cases}$$

for z being the vertex or midpoint of each edge.

Proof. We only prove the case for NRQ_1^a, the case for the five-point NRQ_1 may be proceeded similarly.

For z being the element center, the estimate is a direct consequence of Theorem 3.1.

While for z being the vertex or midpoint of each edge, since $\mathcal{T}_h$ satisfies the *Condition* (β, σ), we may decompose $Z = Z_1 \cup Z_2$, where

$$Z_i \colon = \{\, z \in Z \mid z \in \Omega_{1,h} \,\} \quad i = 1, 2.$$

Therefore, using Theorem 3.1, we have

$$\begin{aligned} \|\overline{\nabla}(u - u_h)(z)\|_{\ell^2} &= (\#Z)^{-1/2}\Big(\sum_{z \in Z_1} |\,\overline{\nabla}(u - u_h)(z)\,|^2 + \sum_{z \in Z_2} |\,\overline{\nabla}(u - u_h)(z)\,|^2\Big)^{1/2} \\ &\leq C(\#Z_1/\#Z)^{1/2}(h^{2\alpha}|\ln h\,| + h^{\alpha+\beta}) + C(\#Z_2/\#Z)^{1/2} h|\ln h\,| \\ &\leq C(h^{2\alpha}|\ln h\,| + h^{\alpha+\beta} + h^{1+\sigma/2}|\ln h\,|), \end{aligned}$$

where we have used $(\#Z_1/\#Z) \leq C$ and $(\#Z_2/\#Z) \leq Ch^\sigma$. □

Remark 3.6. *We did not prove a similar result for NRQ_1^p, however, we are apt to conclude that Theorem 3.1 and Corollary 3.5 are also valid for NRQ_1^p by numerics in the next section.*

4. Numerical Results and Discussion

In this section, we report on numerical results for NRQ_1^a, NRQ_1^p and the five-point NRQ_1 element on three sequences of meshes: the Bi-section mesh, which is obtained by applying the bisection refined strategy to the domain, the Kershaw mesh [10]; and a pedagogic trapezoid mesh. For the Kershaw mesh and the trapezoid mesh, we solve the Dirichlet problem (2.1) in the unit square $[0,1]^2$ with the coefficients

$$a_{11} = 1 + x^2,\ a_{12} = a_{21} = xy,\ a_{22} = 1 + y^2, \tag{4.1}$$

and f is chosen so that the exact solution is

$$u(x, y) = x(1 - x)\sin(\pi y).$$

As to the Bi-section mesh, we solve the problem (2.1) in

$$\Omega = \{\, (x,y) \mid 0 \le x \le 1/2, 0 \le y \le 1 \,\} \cup \{\, 1/2 \le x \le 1 \mid 2x - 1 \le y \le 1 \,\}$$

with the same coefficients as (4.1), and f is taken so that the exact solution is

$$u(x,y) = x(y - 2x + 1)\sin(\pi y).$$

Here follows are three sequences of meshes we employed in the computation.

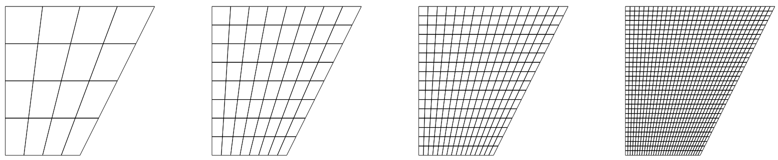

FIGURE 2. Bi-section Mesh

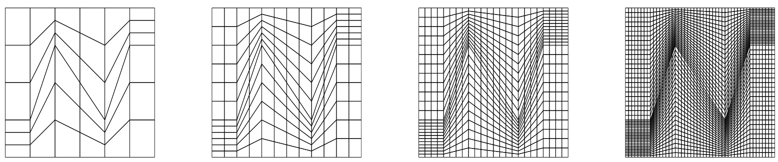

FIGURE 3. Kershaw Mesh

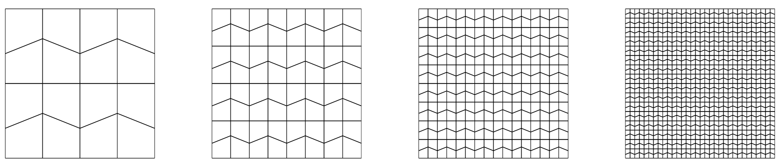

FIGURE 4. Trapezoid Mesh

We list the corresponding values of α, β and σ for three meshes in the following table.

mesh	α	β	σ
Bi-section	1	1	$+\infty$
Kershaw	1	1	1
Trapezoid	0	0	0

TABLE 1. Mesh quality indicators for three meshes

error	$n = 4$	$n = 8$	$n = 16$	$n = 32$	$n = 64$	rate
vertex	$1.19e-1$	$3.44e-2$	$9.06e-3$	$2.32e-3$	$5.85e-4$	1.98
midpoint	$6.69e-2$	$1.81e-2$	$4.63e-3$	$1.17e-3$	$2.95e-4$	1.99
center	$2.63e-2$	$6.51e-3$	$1.63e-3$	$4.07e-4$	$1.02e-4$	1.99

TABLE 2. NRQ_1^a on Bi-section mesh

error	$n = 6$	$n = 12$	$n = 24$	$n = 48$	$n = 96$	rate
Vertex	$1.90e-1$	$8.95e-2$	$3.44e-2$	$1.24e-2$	$4.43e-3$	1.49
midpoint	$1.57e-1$	$6.81e-2$	$2.53e-2$	$8.98e-3$	$3.1653e-3$	1.50
center	$9.97e-2$	$3.30e-2$	$9.20e-3$	$2.39e-3$	$6.04e-4$	1.98

TABLE 3. NRQ_1^a on Kershaw mesh

4.1. Numerics in discrete ℓ_2 norm. In this subsection, we measure the error by the ℓ_2 norm. The numerical results for NRQ_1^a are presented in Table 2, Table 3 and Table 8, respectively. Using the corresponding values of α, β and σ in Table 1, these results confirm the theoretic prediction: Corollary 3.5.

As to the five-point NRQ_1, we list the results on the Bi-section mesh and the Kershaw mesh in Table 4 and Table 5, respectively. By Table 1, these results confirm Corollary 3.5: For the element center, a second order convergence is observed for both meshes, while for the vertex and the mid-point of each edge, a second order convergence is retained over the Bi-section mesh, whereas $3/2-$order convergence is obtained for the Kershaw mesh.

error	$n = 4$	$n = 8$	$n = 16$	$n = 32$	$n = 64$	rate
vertex	$1.15e-1$	$3.28e-2$	$8.59e-3$	$2.19e-3$	$5.54e-4$	1.98
midpoint	$6.46e-2$	$1.71e-2$	$4.37e-3$	$1.10e-3$	$2.77e-4$	1.99
center	$2.71e-2$	$6.68e-3$	$1.67e-3$	$4.17e-4$	$1.04e-4$	2.00

TABLE 4. five-point NRQ_1 on Bi-section mesh

error	$n = 6$	$n = 12$	$n = 24$	$n = 48$	$n = 96$	rate
vertex	$2.21e-1$	$9.39e-2$	$3.58e-2$	$1.30e-2$	$4.69e-3$	1.48
midpoint	$1.72e-1$	$7.17e-2$	$2.65e-2$	$9.47e-3$	$3.35e-3$	1.49
center	$7.79e-2$	$2.80e-2$	$7.74e-3$	$2.01e-3$	$5.08e-4$	1.98

TABLE 5. five-point NRQ_1 on Kershaw mesh

Our theoretic results do not cover NRQ_1^p, however, the following numerics suggest that this element shares the same superconvergence property as NRQ_1^a, which we shall explore in a forthcoming paper. We list the results on the Bi-section mesh, and the Kershaw mesh in Table 6 and Table 7 below. Table 8 shows the numerics on the trapezoid mesh.

4.2. Numerics in maximum norm. In this subsection, we present the numerics in the maximum norm. We still consider problem (2.1) with coefficients (4.1). The right-hand side f is taken such that the exact solution is $\sin(\pi x)\sin(\pi y)y(1-y)$

error	$n=4$	$n=8$	$n=16$	$n=32$	$n=64$	rate
vertex	$1.39e-1$	$4.12e-2$	$1.09e-2$	$2.77e-3$	$6.98e-4$	1.98
midpoint	$7.66e-2$	$2.17e-2$	$5.63e-3$	$1.43e-3$	$3.59e-4$	1.99
center	$4.95e-2$	$1.24e-2$	$3.10e-3$	$7.76e-4$	$1.94e-4$	2.00

TABLE 6. NRQ$_1^p$ on Bi-section mesh

error	$n=6$	$n=12$	$n=24$	$n=48$	$n=96$	rate
vertex	$1.84e-1$	$8.80e-2$	$3.41e-2$	$1.24e-2$	$4.42e-3$	1.49
midpoint	$1.52e-1$	$6.71e-2$	$2.51e-2$	$8.93e-3$	$3.15e-3$	1.50
center	$9.69e-2$	$3.35e-2$	$9.43e-3$	$2.46e-3$	$6.25e-4$	1.98

TABLE 7. NRQ$_1^p$ on Kershaw mesh

error	$n=4$	$n=8$	$n=16$	$n=32$	$n=64$	rate
NRQ1^a	$1.87e-1$	$9.53e-2$	$4.98e-2$	$2.87e-2$	$2.03e-2$	
NRQ1^p	$1.90e-1$	$9.64e-2$	$5.04e-2$	$2.90e-2$	$2.04e-2$	
five-point	$1.85e-1$	$9.28e-2$	$4.65e-2$	$2.33e-2$	$1.17e-2$	0.99

TABLE 8. Numerics on trapezoid mesh

We employ the following maximum norm to measure the error:

$$|\,\overline{\nabla}(u-u_h)(p)\,| = |\,\overline{\partial}_x(u-u_h)(p)\,| + |\,\overline{\partial}_y(u-u_h)(p)\,|.$$

We choose nine special points in Figure 5. This mesh is refined by the bisection strategy, so it automatically satisfies the *Bi-section condition*, i.e., $\alpha = 1$. Moreover, for points $1, 2, 4, 5$ and 7, we have $\beta_K = 0$, while for points $3, 6, 8$ and 9, we have $\beta_K = 1$. Table 10, Table 12 and Table 14 confirm the theoretic prediction (3.2): a first order convergence is observed for points $1, 2, 4, 5$ and 7, while a second order convergence is observed for points $3, 6, 8$ and 9.

error	$n=12$	$n=24$	$n=48$	$n=96$	$n=192$
P_1	$1.14e-1$	$8.00e-3$	$8.53e-3$	$5.52e-3$	$3.09e-3$
P_2	$4.22e-1$	$2.86e-1$	$1.54e-1$	$7.87e-2$	$3.93e-2$
P_3	$5.95e-2$	$1.57e-2$	$3.97e-3$	$9.94e-4$	$2.49e-4$
P_4	$3.36e-1$	$1.46e-1$	$6.70e-2$	$3.13e-2$	$1.52e-2$
P_5	$1.64e-1$	$6.38e-2$	$2.86e-2$	$1.44e-2$	$7.43e-3$
P_6	$6.44e-3$	$2.47e-3$	$6.66e-4$	$1.70e-4$	$4.36e-5$
P_7	$4.68e-2$	$2.15e-2$	$1.57e-2$	$9.09e-3$	$4.93e-3$
P_8	$3.64e-2$	$9.78e-3$	$2.46e-3$	$6.17e-4$	$1.32e-4$
P_9	$1.90e-1$	$4.92e-2$	$1.28e-2$	$3.18e-3$	$8.07e-4$

TABLE 9. NRQ$_1^a$: $|\overline{\nabla}(u-u_h)(p)|$ on Kershaw mesh

rate	$12-24$	$24-48$	$48-96$	$96-192$
P_1	3.8367	-0.0923	0.6289	0.8349
P_2	0.5614	0.8884	0.9719	1.0038
P_3	1.9252	1.9810	1.9964	1.9990
P_4	1.2029	1.1235	1.0980	1.0400
P_5	1.3598	1.1582	0.9841	0.9589
P_6	1.3833	1.8893	1.9724	1.9637
P_7	1.1237	0.4533	0.7877	0.8833
P_8	1.8980	1.9891	1.9987	2.2212
P_9	1.9496	1.9414	2.0074	1.9806

TABLE 10. NRQ_1^a: superconvergence rate on Kershaw mesh

error	$n=12$	$n=24$	$n=48$	$n=96$	$n=192$
P_1	$2.81e-1$	$8.82e-2$	$3.60e-2$	$1.68e-2$	$8.09e-3$
P_2	$5.43e-2$	$6.31e-2$	$3.83e-2$	$2.04e-2$	$1.01e-2$
P_3	$5.25e-2$	$1.35e-2$	$3.40e-3$	$8.53e-4$	$2.13e-4$
P_4	$2.88e-1$	$9.97e-2$	$4.10e-2$	$1.81e-2$	$8.44e-3$
P_5	$1.42e-1$	$6.57e-2$	$3.13e-2$	$1.47e-2$	$7.29e-3$
P_6	$9.86e-3$	$2.19e-3$	$5.62e-4$	$1.41e-4$	$3.54e-5$
P_7	$6.56e-2$	$5.63e-2$	$3.61e-2$	$2.02e-2$	$1.07e-2$
P_8	$2.64e-2$	$7.25e-3$	$1.84e-3$	$4.60e-4$	$1.02e-4$
P_9	$1.20e-1$	$3.47e-2$	$8.89e-3$	$2.21e-3$	$5.61e-4$

TABLE 11. five-point NRQ_1: $|\overline{\nabla}(u-u_h)(p)|$ on Kershaw mesh

$rate$	$12-24$	$24-48$	$48-96$	$96-192$
P_1	1.6716	1.2952	1.0973	1.0540
P_2	-0.2166	0.7187	0.9123	1.0065
P_3	1.9611	1.9869	1.9971	1.9997
P_4	1.5319	1.2837	1.1747	1.1043
P_5	1.1149	1.0686	1.0923	1.0122
P_6	2.1673	1.9643	1.9990	1.9901
P_7	0.2204	0.6405	0.8359	0.9136
P_8	1.8669	1.9817	1.9964	2.1759
P_9	1.7868	1.9676	2.0048	1.9781

TABLE 12. five-point NRQ_1: superconvergence rate on Kershaw mesh

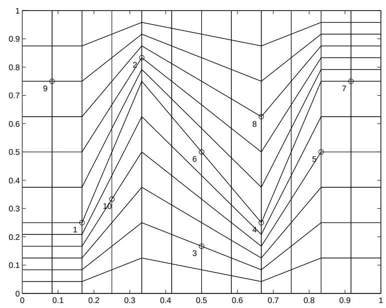

FIGURE 5. Location of the above nine points on Kershaw mesh

error	$n = 12$	$n = 24$	$n = 48$	$n = 96$	$n = 192$
P_1	$1.54e-1$	$1.20e-2$	$7.00e-3$	$5.98e-3$	$3.49e-3$
P_2	$4.35e-1$	$2.88e-1$	$1.55e-1$	$7.86e-2$	$3.95e-2$
P_3	$4.82e-2$	$1.28e-2$	$3.25e-3$	$8.15e-4$	$2.04e-4$
P_4	$3.59e-1$	$1.50e-1$	$6.72e-2$	$3.11e-2$	$1.51e-2$
P_5	$1.34e-1$	$6.27e-2$	$3.57e-2$	$1.81e-2$	$9.05e-3$
P_6	$6.66e-3$	$2.65e-3$	$7.42e-4$	$1.91e-4$	$4.96e-5$
P_7	$6.62e-2$	$3.82e-2$	$2.28e-2$	$1.23e-2$	$6.39e-3$
P_8	$3.69e-2$	$1.02e-2$	$2.60e-3$	$6.54e-4$	$1.64e-4$
P_9	$1.78e-1$	$4.67e-2$	$1.22e-2$	$2.98e-3$	$7.42e-4$

TABLE 13. NRQ$_1^p$: $|\overline{\nabla}(u - u_h)(p)|$ on Kershaw mesh

Rate	$12-24$	$24-48$	$48-96$	$96-192$
P_1	3.6847	0.7735	0.2267	0.7767
P_2	0.5939	0.8981	0.9750	0.9948
P_3	1.9134	1.9770	1.9952	1.9978
P_4	1.2443	1.1567	1.1132	1.0452
P_5	1.0976	0.8113	0.9782	1.0027
P_6	1.3305	1.8356	1.9556	1.9469
P_7	0.7936	0.7421	0.8893	0.9462
P_8	1.8551	1.9713	1.9937	1.9975
P_9	1.9279	1.9392	2.0323	2.0052

TABLE 14. NRQ$_1^p$: superconvergence rate on Kershaw mesh

References

[1] R. A. Adams and J. F. Fournier, Sobolev Spaces, Academic Press, (2-ed), 2003.
[2] T. Arbogast and Z. Chen, On the implementation of mixed methods as nonconforming methods for second-order elliptic problems, Math. Comp. **64** (1995), 943–972.
[3] D. N. Arnold, D. Boffi and R. S. Falk, Approximation by quadrilateral elements, Math. Comp. **71** (2002), 909–921.
[4] Z. Cai, J. Douglas, J. E. Santos, D. Sheen, and X. Ye, Nonconforming quadrilateral finite elements: a correction, Calcolo. **37** (2000), 253–254.
[5] C. M. Chen, Correction of bilinear finite element, Acta Math. Sci. **11** (1990), 13–19.
[6] P. G. Ciarlet, The Finite Element Method for Elliptic Problems. North Holland, Amsterdam. 1978.
[7] J. Douglas, J. J. Santos, D. Sheen and X. Ye, Nonconforming Galerkin methods based on quadrilateral elements for second order elliptic problem, RAIRO. Math. Model and Numer. Anal. **33** (1999), 447–470.
[8] R. Ewing, M. Liu and J. P. Wang, Superconvergence for mixed methods over quadrilaterals, SIAM J. Numer. Anal. **36** (1999), 772–787.
[9] H. Han, A finite element approximation of Navier-Stokes equations using nonconforming elements, J. Comp. Math. **2** (1984), 77–84.
[10] D. Kershaw, Differencing of the diffusion equation in Lagrangian hydrodynamics, J. Comp. Phy. **39** (1981), 375–395.
[11] P. Klouček, B. Li and M. Luskin, Analysis of a class of nonconforming finite elements for crystalline microstructures, Math. Comp. **65** (1996), 1111–1135.
[12] P. Klouček and F. R. Toffoletto, The three dimensional nonconforming finite element solution of the Chapman-Ferraro problem, J. Comp. Phy. **150** (1999), 549-560.
[13] B. Li and M. Luskin, Nonconforming finite element approximation of crystalline microstructures, Math. Comp. **67** (1998), 917–946.

[14] Q. Lin, L. Tobiska and A. Zhou, *On the superconvergence of nonconforming low order finite elements applied to Poisson equation*, IMA J. Numer. Anal. **25** (2005) 160–181.

[15] P. B. Ming, Nonconforming element vs locking problem, Ph. D thesis, CAS, 1999.

[16] P. B. Ming and Z.-C. Shi, Nonconforming rotated Q_1 finite element for Reissner-Mindlin plate, Math. Models Methods. Appl. Sci. **11** (2001), 1311–1342.

[17] P. B. Ming and Z.-C. Shi, Convergence analysis for quadrilateral rotated Q_1 element, In Advances in Computation: Theory and Practice, (P. Minev and Y. P. Ling eds.), Nova Science Publishers, Inc, 2001, 115–124.

[18] P. B. Ming and Z.-C. Shi, Quadrilateral mesh revisited, Comput. Methods Appl. Mech. Engrg. **191** (2002), 5671–5682.

[19] P. B. Ming and Z.-C. Shi, Two nonconforming quadrilateral elements for the Reissner-Mindlin plate, Math. Models Methods. Appl. Sci., to appear.

[20] P. B. Ming, Z.-C. Shi. and Y. Xu, Accuracy of quadrilateral Q_1^{rot} element over irregular mesh, preprint, 2004.

[21] R. Rannacher and S. Turek, Simple nonconforming quadrilateral Stokes element, Numer. Meth. for PDEs. **8** (1992), 97–111.

[22] U. Risch, Superconvergence of a nonconforming low order finite element, Appl. Numer. Math. **54** (2005), 324-338.

[23] Z.-C. Shi, A convergence condition for the quadrilateral Wilson element, Numer. Math. **44** (1984), 349–361.

[24] M. Styness and L. Tobiska, The streamline-difffusion method for nonconforming $Q_1^{\mathrm{rot}}-$ elements on rectangular tensor product meshes, IMA J. Numer. Anal. **21** (2001), 123–142.

[25] S. Turek, Efficient Solvers for Incompressible Flow Problems: An Algorithmic and Computational Approaches, Springer-Verlag, Berlin-New York, 1999.

[26] J. Xu and Z. Zhang, Analysis of recovery type a posteriori error estimators for mildly structured grids, Math. Comp. **73** (2004), 1139–1152.

[27] M. Zlámal, Superconvergence and reduced integration in finite element method, Math. Comp. **32** (1978), 663–685.

Institute of Computational Mathematics and Scientific/Engineering Computing, Chinese Academy of Sciences, No. 55. Zhong-Guan-Cun East Road, Beijing, 100080, China

E-mail: `mpb@lsec.cc.ac.cn, shi@lsec.cc.ac.cn, yunxu@lsec.cc.ac.cn`